

A Physically Based Terrain Morphology and Vegetation Structural Classification for Wetlands of the Boreal Plains, Alberta, Canada

Laura Chasmer, Christopher Hopkinson, Joshua Montgomery & Richard Petrone

To cite this article: Laura Chasmer, Christopher Hopkinson, Joshua Montgomery & Richard Petrone (2016) A Physically Based Terrain Morphology and Vegetation Structural Classification for Wetlands of the Boreal Plains, Alberta, Canada, Canadian Journal of Remote Sensing, 42:5, 521-540, DOI: [10.1080/07038992.2016.1196583](https://doi.org/10.1080/07038992.2016.1196583)

To link to this article: <http://dx.doi.org/10.1080/07038992.2016.1196583>



Accepted author version posted online: 03 Jun 2016.
Published online: 03 Jun 2016.



Submit your article to this journal [↗](#)



Article views: 102



View related articles [↗](#)



View Crossmark data [↗](#)



Citing articles: 1 View citing articles [↗](#)

A Physically Based Terrain Morphology and Vegetation Structural Classification for Wetlands of the Boreal Plains, Alberta, Canada

Laura Chasmer^{1,*}, Christopher Hopkinson¹, Joshua Montgomery¹,
and Richard Petrone²

¹*Department of Geography, University of Lethbridge, 4401 University Drive, Lethbridge, Alberta T1K 3M4, Canada*

²*Geography and Environmental Management, University of Waterloo, Waterloo, Ontario N2L 3G1, Canada*

Abstract. The objective of this study is to test a cost-effective, physically based Light Detection and Ranging (LiDAR) classification methodology for wetland and upland land cover types within an area exceeding 1,000 km² in the Boreal Plains, Alberta, Canada. Decision criteria are based on physical attributes of the landscape that influence maintenance of land cover types. Results are compared with 38 geolocated measurement plots at land cover boundaries and transition zones, manual delineation of 2,337 wetlands using photogrammetric methods and publicly available land cover classifications.

Results suggest that 57% of LiDAR-based wetland classes correspond with delineated wetlands, whereas 37% occur as errors of commission due to excluded wetlands in the manual delineation and confusion with harvested areas. Comparison of classified edges with plot shows that all classifications underestimate wetland area. Residual differences of the LiDAR-based classification are –0.3 m, on average (compared with measured), and have reduced range of error compared with other methods. Multispectral classifications misclassify up to 2/3 of wetland boundaries as a result of lower-resolution mixed pixels. Therefore, high-resolution maps of terrain morphology and vegetation structure provide an accurate, cost-effective means for characterizing wetland vs. upland forest in areas where LiDAR data are available.

Résumé. L'objectif de cette étude est de tester une méthode de classification à partir du lidar «Light Detection and Ranging (LiDAR)», qui est économique et basée sur la physique, pour les types de couvertures terrestres des zones humides et des hautes terres dans une zone de plus de 1,000 km² dans les plaines boréales, en Alberta, au Canada. Les critères de décision sont basés sur les attributs physiques du paysage qui influencent le maintien des types de couvertures terrestres. Les résultats sont comparés avec 38 parcelles de mesure géolocalisées aux frontières de couverture terrestre et de zones de transition, la délimitation manuelle des 2,337 zones humides en utilisant des méthodes de photogrammétrie et les classifications de la couverture terrestre accessibles publiquement.

Les résultats suggèrent que 57 % des zones humides classées à partir du lidar correspondent aux zones humides définies, tandis que 37 % sont des erreurs de commission en raison de zones humides exclues dans la délimitation manuelle et la confusion avec des zones récoltées. La comparaison des bords classés avec les parcelles montre que toutes les classifications sous-estiment la superficie de la zone humide. Les différences résiduelles de la classification à partir du lidar sont de –0.3 m, en moyenne (par rapport à la mesure) et ont une marge d'erreur réduite par rapport à d'autres méthodes. Les classifications multispectrales ont mal classé jusqu'à 2/3 des limites de zones humides en raison de la résolution plus basse des pixels mixtes. Par conséquent, les cartes de haute résolution de la morphologie du terrain et de la structure de la végétation fournissent un moyen précis et économique pour la caractérisation des zones humides par rapport à la forêt des hautes terres dans les zones où les données lidars sont disponibles.

INTRODUCTION

Canadian wetlands, defined as saturated areas of land containing waterlogged and altered soils, and water tolerant vegetation (Government of Alberta 2013) comprise approximately 14% of the land area of Canada (Environment Canada 2016).

Despite their broad areal coverage, these sensitive ecosystems are declining at a staggering rate. In Alberta, approximately 2/3 of wetlands found in settled parts of the province no longer exist, mainly as a result of agricultural drainage and urban development (Government of Alberta 2013). Within “natural” and crown land areas of Alberta, rates of boreal wetland change have not been accurately quantified. This is of grave concern because Canada has one of the greatest rates of boreal forest disturbance globally (78% by 2008; Komers and Stanojevic 2013), due to

Received 16 October 2015. Accepted 8 February 2016.

*Corresponding author e-mail: laura.chasmer@uleth.ca.

natural resources extraction, land cover change/agriculture and natural disturbance (de Groot et al. 2013). In addition to disturbance, severe drying as a result of warmer air temperatures and reduced/stable precipitation over the last 30+ years might have intensified ecosystem sensitivity to climate change and disturbance, potentially creating a “tipping point” scenario of surface/groundwater drying for many wetland/inland pond ecosystems. Such trends have already been identified in many northern parts of Canada and Alaska, resulting in changes to hydrology, vegetation succession, and increased respiration and methane production (e.g., Roulet 2000; Sturm et al. 2001; Stow et al. 2004; Klein et al. 2005; Riordan et al. 2006; Smith et al. 2014), which, over vast regions, could exacerbate positive feedbacks to the climate system (Tarnocai 2009). As a result, accurate classification of wetland type and occurrence is fundamentally important for understanding global environmental change and implementation of sound political decisions with regard to wetland disturbance and reclamation.

Quantifying changes to boreal wetland ecosystems can be difficult but is required to monitor wetland conservation and change. Traditional mapping requires intensive in situ data collection of species type/taxonomy and visual assessments of percent species cover (e.g., Halsey et al. 2003). Methods are often costly and time consuming, and sites might be inaccessible. Remote sensing technologies offer an alternative for large-area mapping of wetlands/forest transition zones through continuous observation of Earth’s surface (e.g., Ozesmi and Bauer 2002). However, the criteria used to classify wetlands differ among data products. In some global vegetation datasets, small and perennial wetlands might be missed entirely within large pixels containing mixed land cover types (Frey and Smith 2007; Krankina et al. 2008) or may be aggregated into other classes within global land cover data products (Krankina et al. 2008). Mixed pixels and aggregation of land cover types often results in significant underestimation of wetland extent and type (Frey and Smith 2007). Krankina et al. (2008) use the example of peatlands (bogs, swamps, fens) to describe differences in classification criteria. They found that optical remote sensing methods were not able to directly measure some of the defining characteristics of peatlands, specifically, an accumulated layer of peat exceeding a depth of 40 cm found on organic, waterlogged soils (National Wetlands Working Group 1997). Therefore, peatland mapping requires the use of proxy variables often including surface hydrology, geomorphological land surface features, and floristic characteristics, which might or might not be consistent across all wetlands at all times or over broad regions (e.g., Frey and Smith 2007).

Numerous studies have demonstrated the use of airborne Light Detection and Ranging (LiDAR) for automated detection of wetland edges, types, and characteristics, using LiDAR only (Korpela et al. 2009; Richardson et al. 2010), LiDAR/synthetic aperture radar fusion (Knight et al. 2013; Millard and Richardson 2013), and LiDAR/optical fusion (Gilmore et al. 2008;

Krankina et al. 2008; Chasmer et al. 2014) methods. LiDAR systems sample 3D attributes of the land surface below and within canopies at high spatial resolution. Most LiDAR-based classifications use proxy indicators of wetland definition mentioned by Krankina et al. (2008), including topographic derivatives such as slope, plan curvature, and profile curvature (e.g., Chasmer et al. 2014). These indicate where wet areas are expected by slight to moderate depressions of the surface compared with surrounding local topography (White et al. 2012). This has led to the development of integrative land surface data derivatives that describe various functions of wetlands to be included within the classification methodology beyond spectral information. Using photogrammetrically derived digital elevation models (DEMs), Hogg and Todd (2007) suggest that spatially explicit variations in topography, vegetation characteristics, and linkages to hydrological feedbacks within the local environment improve the characterization of wetlands, although this adds additional complexity to the classification method. Millard and Richardson (2013) tested 84 LiDAR-based vegetation and topographic derivatives, including those that can be used to define water movement (e.g., topographic wetness index) within a Random Forest classification of a bog and surrounding land cover types in Southern Ontario. They found that 22 data derivatives could be used to characterize the bog and reduced these further to 8 key variables, but ultimately, the standard deviation of all laser returns and the residual of the DEM above/below a polynomial surface provided the greatest explanation of the variance between classes. Unlike Hogg and Todd (2007), they found that slope-related metrics were less important. Hopkinson et al. (2006) also suggest that the standard deviation of all returns provide an important metric for estimating vegetation height for all vegetation types studied and LiDAR survey parameters (i.e., pulse repetition frequency, flying height, etc.), without the need for standardization.

In recent years, the utility of LiDAR for high-resolution mapping of the land surface over broad regions has become a reality (Hopkinson et al. 2013) due to rapid technological innovations and a need for baseline mapping; however, few studies have capitalized on the use of LiDAR data for broad-area mapping of wetlands. In this study, a wetland classification methodology is developed based on LiDAR data derivatives that represent indicators for the existence and maintenance of more than 2,330 wetlands and additional land cover types. The data derivatives used in the classification include indices describing locally topographic high and low areas (topographic morphology), vegetation structural variability, and surface reflectance. To determine whether the classification is valid in areas of variable surficial geology and soil characteristics, methods are applied to an area (study polygon) exceeding 1,000 km² of the Boreal Plains ecozone, Alberta, Canada. Approximately 1/3 of the study polygon consists of a mixture of heterogeneous wetlands and till moraine upland forests (herein described as “Till Moraine”), whereas the other 2/3 consists of geologically homogeneous clay plains

overlain by forests and forest harvest blocks, wetlands, and roads (herein described as “Clay Plains”). The objectives of this study are to

1. evaluate the efficacy of the classification methodology within both Till Moraine and Clay Plains regions by comparing them with a broad-area manual photo delineation of wetland types (herein referred to as “delineated wetlands”) and extents as a best estimate of wetland coverage (Halsey et al. 2004);
2. quantify differences between the LiDAR-based classification and 2 lower-resolution multispectral classifications used by the province of Alberta: (i) a Canada-wide classification: Earth Observation for the Sustainable Development of forests (EOSD: Wulder et al. 2008), and (ii) the Alberta Ground Cover Classification (AGCC: Sánchez-Azofeifa et al. 2004), baseline dataset for land cover assessment in Alberta;
3. validate land cover edge delineation of tested classification methodologies using geographically located vegetation plots at land cover boundaries and transition zones.

Provincial interest in a manually delineated air photo-based wetland dataset indicates that a highly accurate and broad-area methodology is needed for defining wetland ecosystems, extents, and characteristics as they currently exist. The Alberta Wetland Policy (2013) requires: (i) an inventory of all wetlands in a given area as the foundation for the Alberta Wetland Policy; (ii) the ability to assign a value to all wetlands based on biodiversity and ecological health, hydrological function, and relative abundance of wetland types; and (iii) tools for evaluating wetland loss and restoration. With almost wall-to-wall coverage, LiDAR datasets for the Province of Alberta provide unprecedented opportunity to examine and quantify baseline land cover types and to develop methods appropriate for ecozones and underlying land surface characteristics. This methodology provides a timely alternative or complement to currently available optical and RADAR-based products used by the Province of Alberta.

STUDY AREA

The study polygon covers an area of 1,062 km² and is located to the north of Utikuma Lake (56.04, -115.30) ~ 300 km north of Edmonton, Alberta, within the Boreal Plains ecozone of the Canadian boreal forest (Figure 1a). The Utikuma Regional Study Area (URSA) was established as a long-term monitoring site in 1998, primarily to quantify key hydrological processes that have formed ecosystem diversity and resilience across a variety of landscape scales, disturbance regimes, and successive cycles (Ferone and Devito 2004; Petrone et al. 2007). On an annual basis, average air temperature is 0.2°C (Natural Regions Committee 2006) and potential evapotranspiration often exceeds precipitation (Devito et al. 2005), making this region sensitive to warming/drying trends (Petrone et al. 2007). The study polygon is part of the Central Mixedwood subregion of

the Northern Alberta Uplands and consists of a heterogeneous mosaic of upland forests often found on stagnant ice moraines with medium-textured glacial till soils to the west of the polygon (heterogeneous area, Figure 1b; Ferone and Devito 2004). Wetland ecosystems comprise, predominantly, shallow ponds, treed fens, and bogs on poorly drained organic soils (Natural Regions Committee 2006). The eastern part of the study polygon is characterized by gently undulating clay till plain comprising glacio-lacustrine deposits and productive conifer forests (Ferone and Devito 2004).

The height transition between pond and wetland surfaces to riparian and upland mixedwood forests is often abrupt, with surrounding riparian vegetation comprising larch (*Larix laricina*), green alder (*Alnus viridis*), paper birch (*Betula papyrifera*), bog birch (*Betula glandulosa*), and occasional Alaskan birch (*Betula neoalaskana*) on gently increasing elevation found a few meters from the wetland edge (Petrone et al. 2007). Mixedwood upland forests comprise, mainly, aspen (*Populus tremuloides*), white spruce (*Picea glauca*), balsam poplar (*Populus balsamifera*) that rise up to 30 m above the pond/wetland surface in the western (heterogeneous) part of the study area. Black spruce (*Picea mariana*) is found mostly within treed wetlands underlain with *Sphagnum* spp. moss and fibric peat, grasses up to 0.5 m in height, and gyttja hummocks and hollows, whereas open wetlands contain small birch and alder seedlings. Ponds are characterized by submergent macrophyte vegetation that might float on top of ponds in summer (Petrone et al. 2007). In the eastern portion of the study polygon, sand/clay soil increases drainage and encourages jack pine (*Pinus banksiana*) growth. The region is also highly disturbed with significant areas of forest harvesting, oil and gas extraction, and mining.

MATERIALS

Airborne LiDAR Data

Airborne LiDAR data were collected by Airborne Imaging Inc.¹ in late August, 2006, 2007, and early September 2008, using a small footprint discrete return ALTM 3100EA² operated at flying heights near 1,400 m above ground level (Figure 1b). A pulse repetition frequency of 50 kHz and a scan angle of ± 25° was used with 50% overlap between scan lines to reduce minimal occlusion of laser pulses by the canopy and to effectively sample from both sides of tree crowns. Comparison with Moderate resolution Imaging Spectroradiometer (MODIS)-enhanced vegetation index (EVI)³ indicates that phenological changes to vegetation had not occurred until the week of September 29 (for the 2008 survey period acquired in early September).

Quality control processing for high/low returns and removal of areas with greater than 50% overlap of scanlines

¹Calgary, AB; licensed to the Province of Alberta

²Optech Inc., Toronto, Ontario

³Optech Inc., Toronto, Ontario

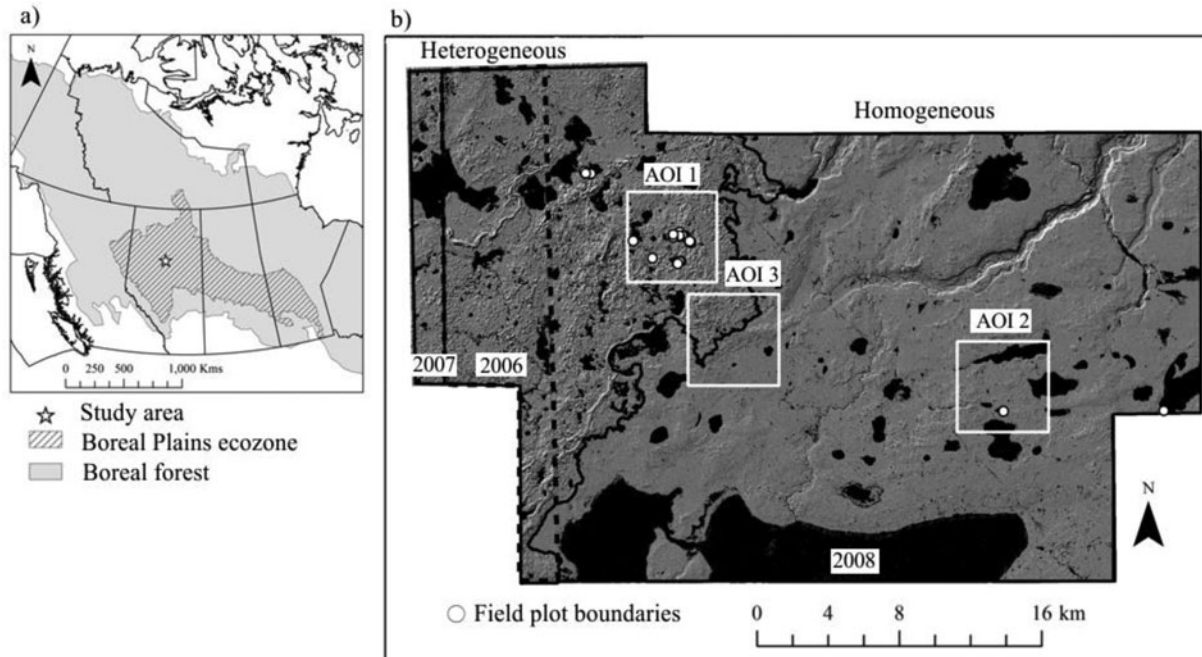


FIG. 1. (a) Location of the $\sim 1000 \text{ km}^2$ study area polygon within the Boreal Plains ecozone, Alberta, Canada. The study polygon (b) is divided by a black line into “Heterogeneous” Till Moraine and “Homogeneous” Clay Plains. LiDAR data subsets were acquired in 2006, 2007, and 2008 displayed as a hillshade model of the original DEMs. Three concentrated areas of interest (AOI) are used for comparison, and the locations of field plots along wetland boundaries are illustrated.

was performed in TerraScan (Terrasolid, Finland). Cutting of overlapping areas reduces increased return reflection within canopies at scan line edges (Morsdorf et al. 2008) and within areas exceeding double overlap. Laser return data were then tiled and classified into ground, nonground and all returns using TerraScan. A $2\text{-m} \times 2\text{-m}$ DEM was created, using an inverse distance weighting (IDW) approach with a search radius of 2.5 m derived from the ground-classified returns. A gridded variance map of all returns was also created within a $2\text{-m} \times 2\text{-m} \times z$ column as the sum of the squared deviations of z (height) from the mean of all returns divided by 1 less than the total number of returns within a column. Finally, laser return intensity was normalized for range and scan angle, using methods of Hopkinson (2007) and Crasto et al. (2015) for paved road surfaces crossing between survey polygons and rasterized to 2 m resolution using the same IDW method. Intensity was also checked, using dark subtraction from lowest intensity pixels. A digital surface model (DSM) and canopy height model ($\text{CHM} = \text{DSM} - \text{DEM}$) were created for visualization (not used in the classification) based on the mean maximum height of all returns found within a $2\text{-m} \times 2\text{-m} \times z$ column.

Comparison Datasets: Delineated Air Photos, AGCC and EOSD

Numerous remote-sensing-based datasets are used for comparison with the LiDAR-derived wetland classification presented in this study. The first method is based on wide-area

aerial photo delineation (herein referred to as “delineated wetlands”;⁴ Figure 2a). A detailed map of wetland extents and types exists for an area covering 42 1:250,000 map sheets. A small subset of this area is compared with the LiDAR-based classification. The purpose of the wetland delineation is to upgrade and improve the peatland/wetland classification system established by the National Wetlands Working Group (1988, 1997; Halsey et al. 2004) and by Vitt et al. (1996; Figure 2a). Wetlands were identified, delineated, and characterized from air photos according to Vitt et al. (1996) by the Alberta Peat Task Force (Halsey et al. 2004), using orthorectified and geometrically corrected aerial photograph mosaics, completed in 2002. The wetland extent shape file contains wetland classes/types, vegetation characteristics, and area attributes in table form per delineated wetland. Delineated wetlands were then subset, rasterized, to 2-m resolution and converted into geotiff for direct comparison with the LiDAR-based wetland classification.

The second dataset compared with the LiDAR-based classification is the publicly available EOSD classification described in Wulder et al. (2007, 2008) as a standard forest land cover product for Canada (Figure 2b). The EOSD product comprises $25 \text{ m} \times 25 \text{ m}$ pixels and 23 land cover classes derived from Landsat multispectral data representing the conditions of the land, circa 2000, following methods of Wulder et al. (2007). Four hierarchical classification levels are used to characterize

⁴Provided by the Devonian Botanic Garden, University of Alberta.

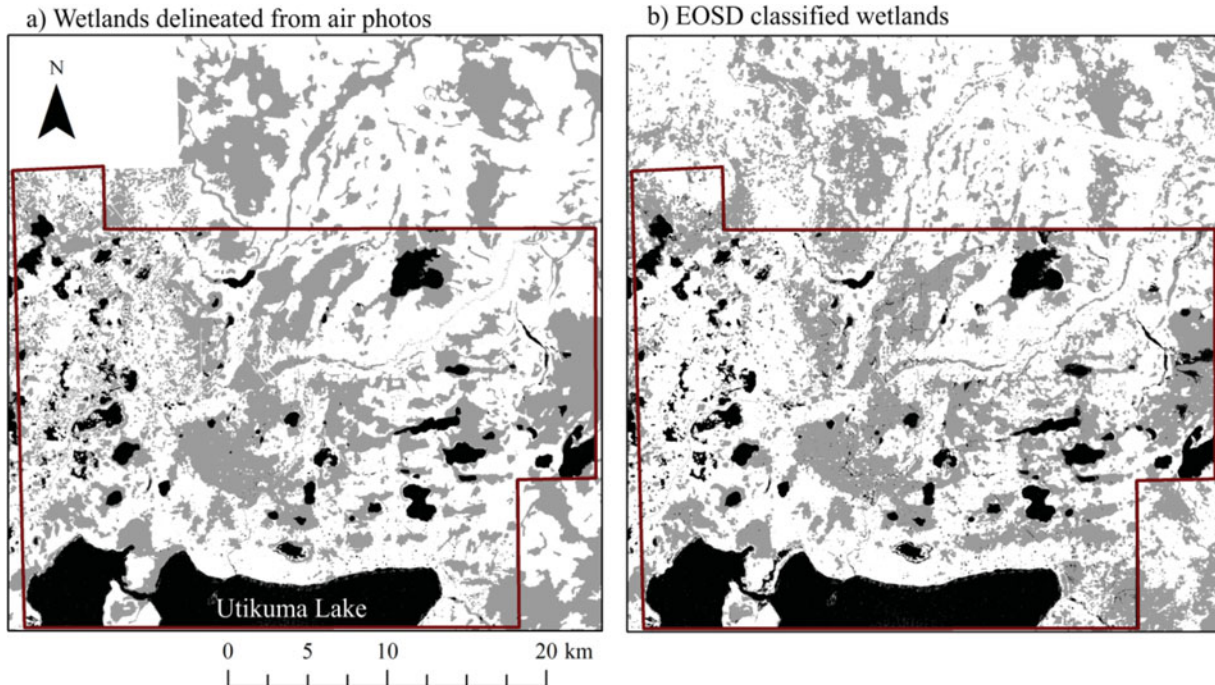


FIG. 2. Combined wetland classes: (a) bog, fen, swamp, marsh, delineated from air photos (Halsey et al. 2004) and (b) grass, shrub, treed wetland classes from the E OSD classification (Wulder et al. 2008), both illustrated in gray for the region north of Utikuma Lake. Lakes are represented in black, the study polygon indicating LiDAR coverage is outlined. For simplicity, AGCC is not shown here due to similarity with E OSD, except when examining small areas of the classified wetlands do differences appear.

increasingly specific characteristics of the land surface, using National Forest Inventory (NFI) protocols. The results of the classification have been validated over Vancouver Island based on plots and airborne video in Wulder et al. (2006 and 2007). Wulder et al. (2006) note producer's accuracies of between approximately 40%–50% within a class of treed, shrub, and herb wetlands. Classes were similarly combined in this study and re-sampled to 2 m resolution for comparison of all wetlands within the original treed wetland, shrub wetland, and grass wetland classes.

Finally, the Alberta Ground Cover Classification (AGCC) is an additional, publicly available land cover classification created in partnership by Alberta Environment and Sustainable Resource Development, Government of Alberta, and Agriculture and Agri-Food Canada, circa 2000. The classification uses Landsat 5 and Landsat 7 multispectral data, acquired between August 1999 and 2002, for 51 land cover classes found in Alberta, described in Sánchez-Azofeifa et al. (2005). The classification was designed as a complement to the national E OSD program, and provides 5 increasingly detailed (but also increasingly less accurate) classification levels used to build an unsupervised classification. At Level 2 (defined wetland extent similar that provided by E OSD), the expected accuracy is 90%, and at Level 3 (wetland type) this is reduced to an expected accuracy of 85%, based on users' and producers' accuracies of the confusion matrix.

Field Data Collection for Validation

Geographically located vegetation measurement plots were established at separate land cover transition boundaries between upland forest and wetland ($n = 9$), riparian and wetland ($n = 15$), and pond and wetland ($n = 14$) in 2002, 2008, 2012, and 2015 as part of a larger initiative to map vegetation structural characteristics along transects. Plots were randomly located at 16 different pond/wetland sites (with some plots located on opposite sides of an individual pond or wetland) and were at least 25 m from an adjacent plot of the same land cover/wetland boundary. No single plot has been measured twice. Due to a concentration of field work and research activities in the Till Moraine region, all but 4 plots were located in this area, resulting in a combined assessment of Till Moraine and Clay Plains edge detection.

Validation plots were geographically located using survey-grade GPS, postprocessed to better than 0.1 m accuracy within open wetlands and up to 0.3 m accuracy with longer occupation times (up to 15 minutes) near upland forest boundaries. Plot measurements in 2002 are described in Hopkinson et al. (2005). Similar measurement protocols were followed in 2008 and 2015. Plots (0.5 m along cardinal directions) consisted of percent coverage of short vegetation types (aquatic, grass and herbs, low shrubs and tall shrubs; Ducks Unlimited Canada 2002), maximum canopy height (measured by using a tape measure or staff), and a description of the vegetation characteristics. In 2008 and

2012, land cover type was determined based on vegetation characteristics (2012 surveys ($n = 3$), vegetation types, and land cover class boundary only). Open water boundaries within wetlands were determined at the approximate boundary between dry ground and standing water (despite aquatic vegetation extension into ponds).

Removal of Harvested and Regenerating Forest Stands, Using Landsat TM

Similar to field data collections, we assume little change to the environment over the 6–8 years between LiDAR surveys (in 2006–2008), air photo delineation, and Landsat classified products. However, this is not always the case. Disturbance that occurs between air photo/EOSD classifications and the LiDAR-based classification might increase commission errors between LiDAR-classified and other classification datasets, because cleared areas might be flat and contain grasses and regenerating shrubs that appear indistinguishable from many wetlands but should not be classified as such. Further, changes in pond levels and succession can vary from year to year or over the course of many years. To characterize land cover change as a result of harvesting, fire, oil and gas extraction, etc., we use Landsat 5 Higher Level Science Data Products, processed using the Ecosystem Disturbance Adaptive Processing System (LEDAPS version 2.0). The Modified Soil Adjusted Vegetation Index (MSAVI; Masek et al. 2006) product (path 44, row 21) was accessed using Earth Explorer⁵ for the July 1–August 15 period, 1998, 2001, 2003, and 2008 for cloud-free conditions. Image-to-image normalization of MSAVI was conducted for dark, middle, and light nonvarying, pseudoinvariant features ($n = 136$) following Hall and Hay (2003). Abrupt changes in MSAVI pixels are determined using subtraction (to indicate change), and more gradual slope changes following disturbance are identified and compared with prerule removal classification accuracy.

METHODS

Background

The LiDAR classification described in this study presumes that different parts of the wetland environment have different vegetation structural and topographic or morphological characteristics used to define them, such that the frequency distribution of returns through the canopy can be used as a digital “fingerprint” for the natural environment. For example, Millard and Richardson (2013) observed greater standard deviation of all laser pulse returns within forest environments due to the distribution of returns through the canopy that characterizes this land cover class. They also found reduced standard deviation within bogs containing little/no tall vegetation. Further, Korpela et al. (2009) found that the distribution of returns within vegetation provided strong explanation within a range of diverse

peatlands. Figure 3 demonstrates similarities within and differences between percentile frequency distribution of ground-normalized point clouds related to wetland land cover types and the transition to upland mixedwood. To create structurally different fingerprints of land cover classes used within the classification, point clouds were extracted within 5 m radius plots for 25 representative homogeneous land cover types along measurement transects and 29 randomly sampled locations within the larger study area. Frequency distributions of returns with height were determined per sample location and classified into 6 dominant classes: upland mixedwood, the transition between upland mixedwood and riparian, riparian, wetland, pond, and treed wetland, observed while in the field. For example, upland mixedwood stands are characterized by a large proportion of returns through canopies, with relatively few returns from below canopy and minimal understory vegetation (Hopkinson et al. 2005). They are also typically found on stagnant ice moraines and slightly elevated areas. Toward the outer edges of upland hills, foliage occurs throughout the full canopy profile due to light and moisture regimes and edge influences. This causes reflection of returns throughout the canopy, especially where returns are incident upon and reflect from canopy sides within this transition. The structural characteristics of open wetlands allow for penetration of returns into grasses and sedges to a depth where grasses begin to bend over, creating a less penetrable surface (Hopkinson et al. 2005), reduced standard deviation (Millard and Richardson, 2013), and concentration of returns near the ground surface (Figure 3). Further, reduced DEM accuracy as a result of an inability to penetrate to the ground surface does not demonstrate sufficient variation in variance to put this land cover into a different class (although this could be more problematic in prairie grassland regions).

Friedman’s test on ranks is used to determine if nonparametric differences exist between randomly selected frequency distributions within land cover types, and is used to develop the decision criteria of the LiDAR-based classification. The null hypothesis (H_0) assumes that the frequency distribution of returns within canopies and from the ground surface is the same within land cover types, while the alternative (H_A) suggests that they are different. This provides a rationale based on return variance for differentiating between vegetation structures associated with different land cover types. Except for riparian and treed wetlands, no significant differences between frequency distributions are found within land cover types (P ranges between 0.13 and 0.56 for upland forest, transitional boundaries between forest and riparian, and grass wetland/pond edge, Figure 3). Further, no significant differences are found between those same classes ($P \leq 0.05$, variable Chi sq. depending on comparison), except for treed wetlands and riparian ($P = 0.36$, Chi sq = 10.21) where shrubs and shorter trees have similar distributions of returns between and within vegetated canopies ($P \leq 0.1$, Figure 3). This indicates that some confusion might exist between riparian and treed wetland classes within the overall classification.

⁵ <http://earthexplorer.usgs.gov>

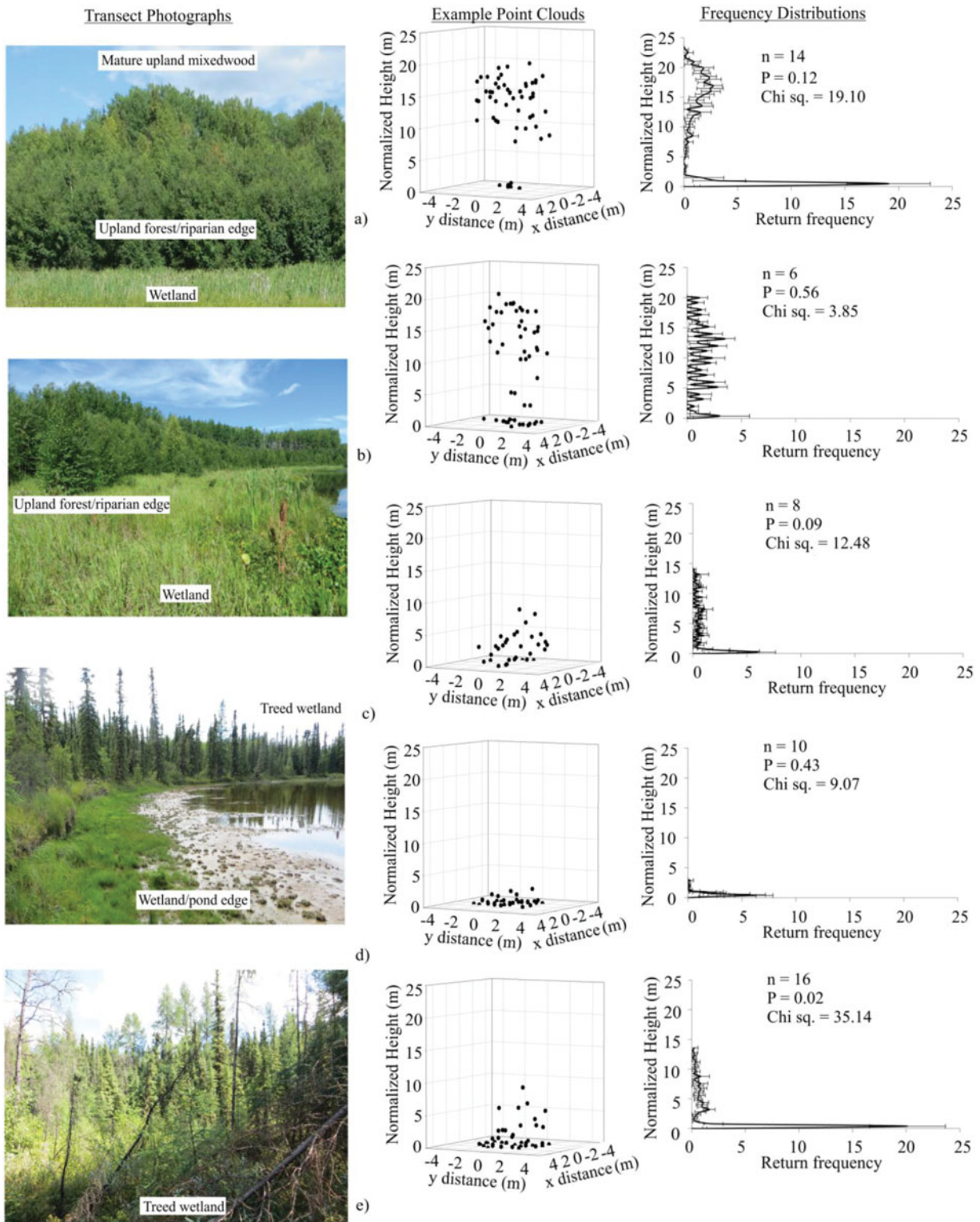


FIG. 3. Representative photographs along transects illustrating different vegetated land cover types used common to natural parts of the Boreal Plains. Example point clouds and frequency distribution with ± 1 standard deviation are also shown for single 5 m radius plots: (a) upland mixedwood forest, (b) transition between upland forest and riparian, (c) riparian, (d) grass wetland/pond edge, and (e) treed wetland.

Airborne LiDAR Classification Methodology

With these fingerprint-type observations in mind, classification procedures are based on the full canopy profile characteristics of the point clouds as a function of the variance of all returns from ground surface to top of canopy. In addition, the residuals from the mean elevation of a predetermined mean surface derived from the ground-classified DEM are used to provide greater differentiation between the ground surface morphology of upland, transition, and wetland classes. The application of a mean surface effectively smooths and removes the underlying topographical trend of the data by placing a plane of mean elevation within a given search radius. The search radius is, therefore, used only to derive a mean DEM surface from which the original DEM can be subtracted. Residual pixel elevation from the original DEMs that occur above and below the mean surface are used to define the locally topographic high and low areas representing uplands and wetland depressions, respectively (Todd and Hogg, 2007; Chasmer et al. 2014). Figure 4 illustrates the procedures used along a single transect crossing pond, wetland, riparian, and upland boundaries.

The circular search radius of the mean elevation is automatically adjusted depending on the standard deviation DEM within a broader region based on the average width of wetlands determined from manual delineation within Till Moraine and Clay Plains regions. Therefore, the heterogeneous Till Moraine region uses a smaller mean elevation search radius (110 m) than the flatter, more homogeneous Clay Plains region (300 m search radius). Classification of roads, cut blocks, and trails is characterized as having low all-return variance due to lack of trees/vegetation found on road and trail surfaces, relatively high-return intensity due to minimal vegetation interception; flat, lightly colored gravel surfaces; road edge DEM slope characteristics; and low standard deviation of all returns. Water is defined following Crasto et al. (2015), using a combination of very low (off nadir/wide scan angles) and saturation (near nadir) normalized intensity. A 3 pixel \times 3 pixel (6 m \times 6 m) majority filter was used to remove intermediate-to-high-return intensities at scan angles slightly off nadir (up to $\pm 6^\circ$), which could be confused with return intensities from roads and wetlands. To avoid expansion/contraction effects of the filter at water edges, water was given lowest priority in the decision criteria (and the other land cover type per pixel would have priority). In addition to Crasto et al. (2015), low standard deviation of all returns compared with other surfaces is used, suggesting flat water surfaces and minimal wave height. Based on ranges of predefined land cover characteristics described, pixels are assigned to a land cover class if they meet the range of criteria defined for that class. The probability of inclusion depends on the number of conditions that have been met for that class. If fewer conditions have been met, then the pixel is assigned to another class. Figure 5 provides a flow diagram of the procedures and characteristic ranges used to define each class.

Comparison of LiDAR Classification with Other Classifications and Field Data

Maps of correspondence, omission, and commission are derived via direct pixel-to-pixel comparisons among the LiDAR-based classification, manually delineated wetlands, AGCC, and EOSD with and without removing previous disturbance and regeneration. Each class-per-product is reclassified into either wetland or nonwetland area, provided with a numeric identifier, and compared, thereby creating a spatially explicit map of classification correspondence beyond more typically used confusion matrices (although these are provided as well). Corresponding codes-per-pixel represent areas where both the LiDAR-based classification and the alternative defined each individual pixel as wetland. Where the LiDAR classification identified a pixel as wetland and the alternative did not, these are presumed errors of commission, whereas the opposite are errors of omission, as long as the alternative classification correctly identifies pixels belonging to wetlands.

Comparisons among validation plots located at approximate land cover boundary edges with wetlands edges defined using LiDAR, photogrammetric, and multispectral classifications were determined based on (i) whether the land cover classification coincides with the location of the plot measurement and (ii) whether the land cover type is accurately classified. If it is not accurately classified (and there are no adjacent or nearby pixels of the same class), then we assume misclassification and the class is given a null value (missing). Where a boundary between land cover and wetland does exist at or near (within 50 m or 2 EOSD/AGCC pixels) the plot measurement boundary location, the linear distance from the plot measurement to the closest pixel edge is recorded in the direction of the adjacent land cover type. If wetland size is underestimated compared with measured (other pixel classes extend into the wetland), then the distance between measured and classified is converted into a negative distance. If the wetland size is overestimated compared with measured, then the distance of wetland extension remains positive. This inherently includes fuzzy transitional boundaries between classes because these are often not abrupt.

RESULTS

Application of the LiDAR-Based Classification to Till Moraine and Clay Plains Regions

The spatial distribution of wetland classes (treed, open, and riparian zones), water, and disturbance using the LiDAR-based classification is presented in Figure 6a with spatial correspondence presented in Figure 6b. The Till Moraine (western) part of the study polygon is characterized by greater proportional coverage of forests (42%), fewer wetlands (47%) and fewer shallow water ponds and lakes (11%) compared with the Clay Plains (eastern) part of the study polygon. However, caution

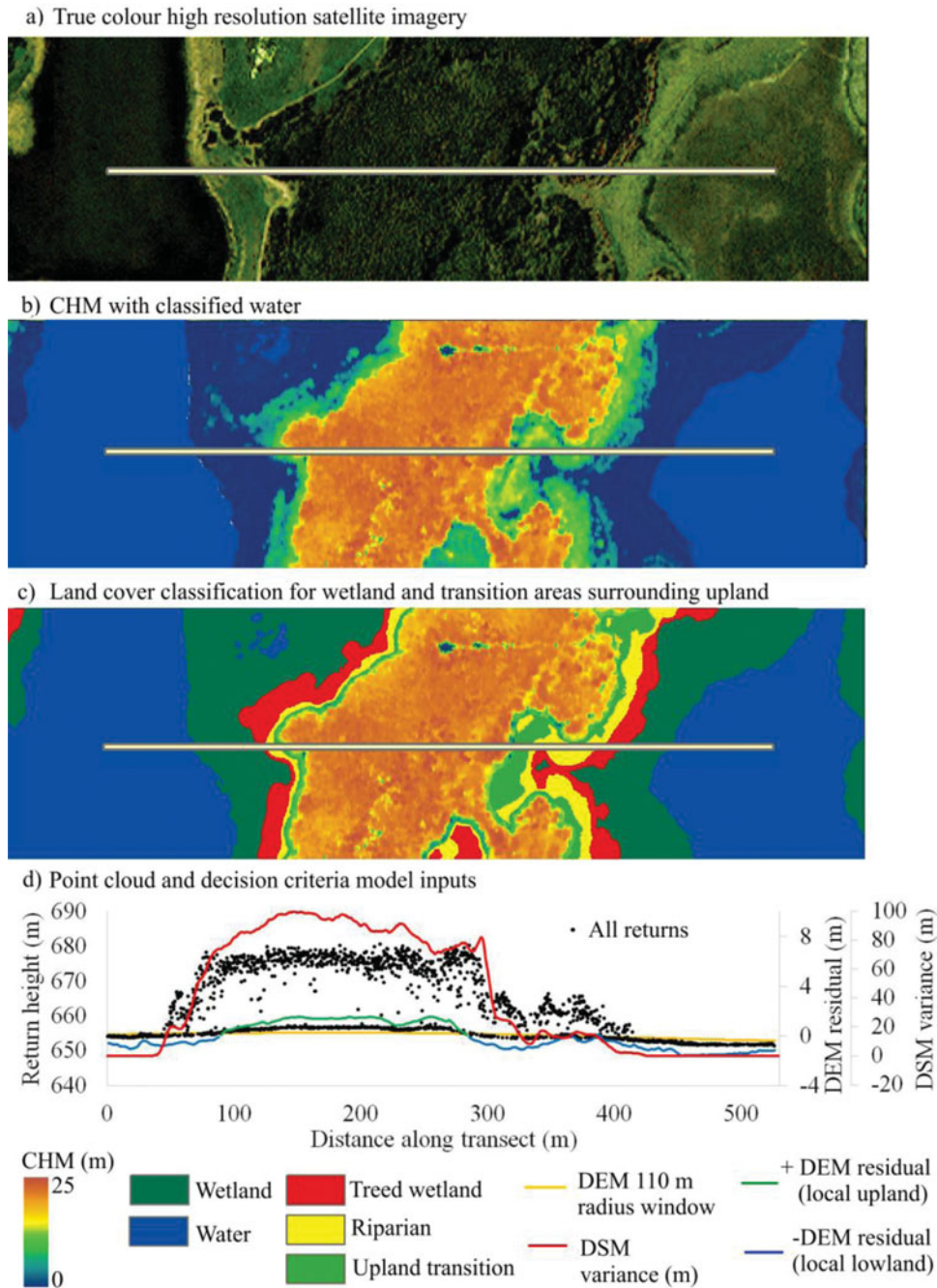


FIG. 4. Diagram illustrating methods used as viewed along a 530-m transect (white line) illustrated through the center of each image: (a) true color high-resolution satellite imagery from WorldView-2 illustrates the transition between pond-wetland-upland forest-wetland and pond classes; (b) shows the same area and transect overlaid onto a canopy height model (CHM = DSM – DEM). Mature upland mixedwood forests range in height between ~ 22 m and 25 m, whereas transitional and riparian vegetation height range is between 4 m and 18 m. Ponds in (b) have been classified. (c) LiDAR-classified wetlands based on topographic residuals and grouped variance in all areas except for upland mixedwood (illustrated as a CHM). (d) A profile view of the 2 m × 530 m all-return point cloud transect, and demonstration of the mean surface, DEM residuals, and all-return variance.

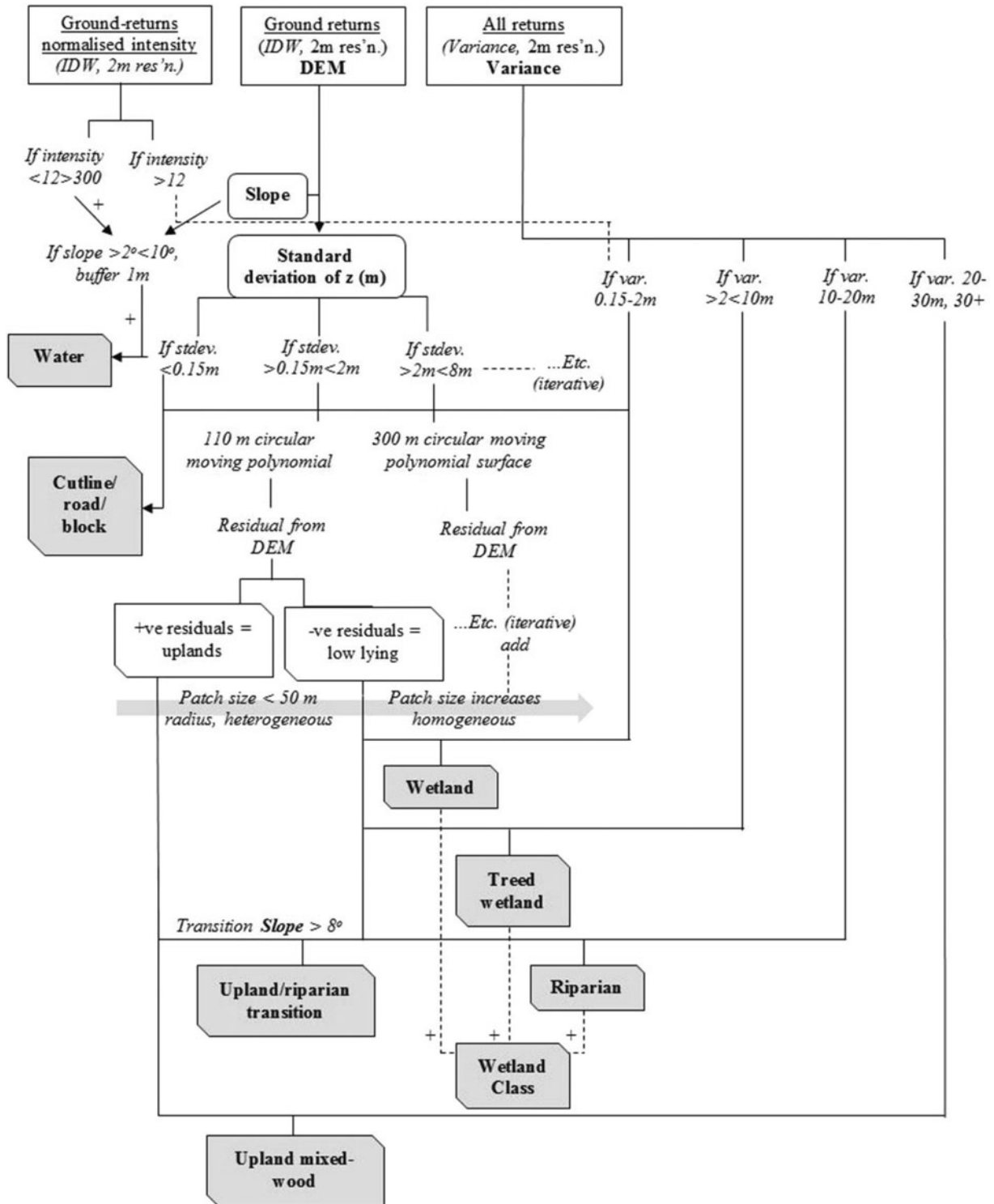


FIG. 5. Flow diagram of classification procedure and defined ranges (in italics). Rectangles indicate inputs, rounded corners are intermediate data derivatives, and gray blocks with blunt corners represent final classes.

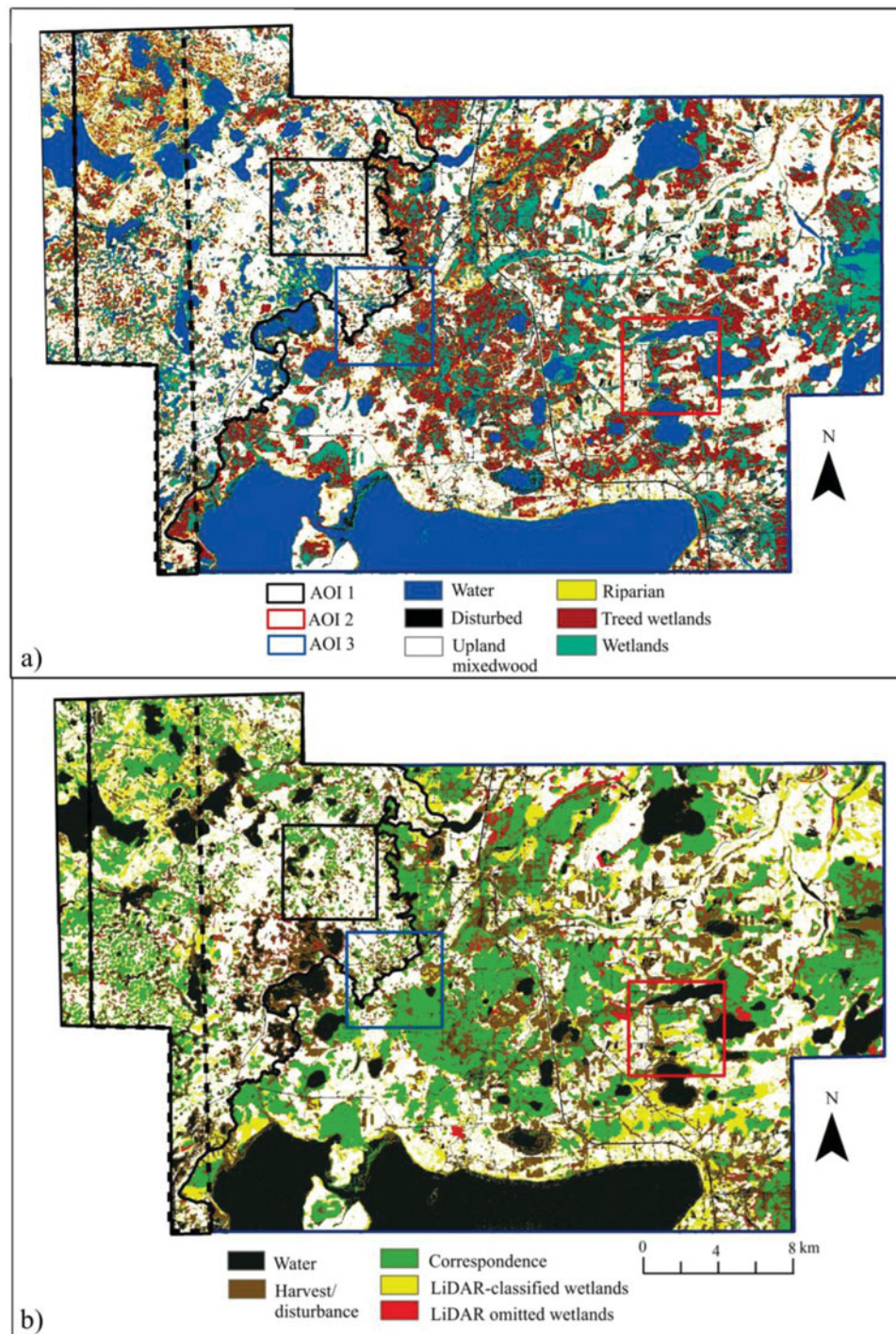


FIG. 6. (a) Classification of water, disturbance (including roads, trails and harvest, but excluding regenerating forests), wetlands and wetland/forest boundaries within LiDAR subsets collected in 2006, 2007, and 2008. (b) Spatial patterns of correspondence, commission errors (yellow) and omission errors (red) between LiDAR-based wetland areas and wetlands delineated using photogrammetric methods.

TABLE 1

Comparison between the LiDAR-based classification of wetlands, and photo-delineated wetlands, EOSD and AGCC both excluding and including harvest and regeneration areas. Correspondence and commission/omission errors have been further divided into LiDAR data vintage subsets (acquired in 2006, 2007, and 2008), and regional analysis within the Clay Plains and Till Moraine parts indicative of more and less landscape heterogeneity

Comparison	LiDAR Collection and Sections	% Corresp. ($\times 100\%$)	% Commission ($\times 100\%$)	% Omission ($\times 100\%$)
LiDAR classification vs. air photo delineated	2006	0.57	0.36	0.07
	2007	0.64	0.29	0.07
LiDAR vs. EOSD	2008	0.57	0.37	0.06
	Clay Plains	0.57	0.38	0.05
	Till Moraine	0.58	0.32	0.10
	Total Wetland Area	0.57	0.37	0.06
	2006	0.52	0.39	0.09
	2007	0.54	0.40	0.06
	2008	0.53	0.41	0.06
	Clay Plains	0.56	0.38	0.06
	Till Moraine	0.46	0.46	0.08
	Total Wetland Area	0.53	0.38	0.09
LiDAR vs. AGCC	2006	0.53	0.38	0.09
	2007	0.50	0.44	0.06
	2008	0.55	0.37	0.08
	Clay Plains	0.57	0.36	0.07
	Till Moraine	0.48	0.44	0.08
	Total Wetland Area	0.54	0.38	0.08
	2006	0.60	0.33	0.07
LiDAR vs. delineated, (corrected for harvest and regeneration (temporal Landsat TM))	2007	0.63	0.30	0.07
	2008	0.63	0.31	0.06
	Clay Plains	0.63	0.32	0.05
	Till Moraine	0.60	0.30	0.10
	Total Wetland Area	0.62	0.32	0.06
	2006	0.60	0.31	0.09
LiDAR vs. EOSD, (corrected for harvest and regeneration)	2007	0.59	0.35	0.06
	2008	0.66	0.28	0.06
	Clay Plains	0.70	0.24	0.06
	Till Moraine	0.55	0.37	0.08
	Total Wetland Area	0.65	0.26	0.09
	2006	0.56	0.35	0.09
LiDAR vs. AGCC, (corrected for harvest and regeneration)	2007	0.48	0.46	0.06
	2008	0.72	0.20	0.08
	Clay Plains	0.76	0.17	0.07
	Till Moraine	0.52	0.40	0.08
	Total Wetland Area	0.67	0.25	0.08

should be used when interpreting these results because they do not consider errors of commission and omission (Figure 6b). Positioning of wetlands in the Till Moraine region is related to underlying geology and hydrologically isolated pond/wetland complexes. Within the Clay Plains region, wetlands and shal-

low ponds dominate the lower elevation region (60%, 29%, respectively). Increased accessibility is also linked to more roads and cutlines (4% of total area in the east vs. 3% in the west), large areas of previously harvested forests, and oil/gas extraction wells.

Comparing LiDAR, Manually Delineated, and Multispectral Classifications of Wetland Area

More than 2,330 manually delineated wetlands were found in the survey polygon, 55% classed as peatlands (bog, fen), 39% as swamp, and the remaining wetlands as comprising marsh, shallow surface water ponds, and lakes. The LiDAR classification corresponds best with manually delineated wetlands (Table 1) and to a lesser extent AGCC and EOSD, due to comparable identification of smaller wetlands and wetland boundaries when compared with delineated wetlands. Slightly better correspondence is also found between AGCC compared with LiDAR-based methods, opposed to EOSD.

When compared with manually delineated wetlands, the LiDAR-based classification identifies 38% (Till Moraine) and 32% (Clay Plains) more wetland area than that defined using air photos. However, identification of wetlands (where they do not exist in the wetland delineation) using the LiDAR-based classification is not necessarily an error. Wetlands are sometimes missed by the manual delineation procedure but are included in the LiDAR classification. Further, some delineated wetland areas also include shallow standing water (small ponds) as wetland. These are classified as water in the LiDAR classification.

In other areas, LiDAR methods incorrectly identify regenerating harvest stands as wetland, resulting in difficulty separating confusion errors in the LiDAR-based classification and excluded wetlands in the manual delineation of air photos. When regenerating stands (determined using Landsat MSAVI) are removed, LiDAR methods continue to identify greater total wetland area, but, compared with manually delineated wetlands found in Till Moraine and Clay Plains regions, this is reduced from 38% to 32% and from 32% to 30%, respectively (Table 1). This indicates that, even after previously harvested stands are removed, differences continue to exist between delineated and LiDAR-based methods (Figure 6b). Another source of confusion occurs between the LiDAR-based classification and manually delineated wetlands that exist along roads, seismic lines, and paths. Within the broader study area, 34% of roads (etc.) are classified as wetlands when compared with the EOSD “exposed land” class. Effects of LiDAR survey subset vintage (2006, 2007, and 2008) do not demonstrate large differences, except for increased difference in wetland correspondence between 2007 and 2008 (up to 11%). This could be due to some foliage loss/flattening of grasses during initial stages of senescence or differences in the heterogeneity and size of wetlands identified by using the different classification methods (Table 1).

Figure 7 shows detailed areas of interest (AOIs), including a Landsat false color composite (FCC), the LiDAR-based classification, and maps of correspondence within Till Moraine and Clay Plains regions. In Figure 7a, 17 prominent wetland ecosystems were excluded by the manual delineation, but were classified as wetlands using the LiDAR-based methods. Lack of correspondence is illustrated as commission error, but these

would be greatly reduced if all wetland boundaries were included in the manual delineation. Similar issues are also found in Figure 7b and c, where 7 and 8 prominent wetland ecosystems are missed by manual delineation. This is complicated by misclassification of regenerating stands in Figure 7b and c. Based on additional delineation from high-resolution optical imagery (WorldView 2 in AOIs 1, 3, SPOT 5 in AOI 2), the proportional areas of missing wetlands are 19%, 38%, and 16%, respectively. LiDAR methods incorrectly classify 5 and 3 regenerating stands (with changes observed using Landsat MSAVI) as wetland. These areas have higher reflectance in near infrared (red channel), identified as slightly brighter (red) areas in the Landsat false color composite, illustrating the need for a separate “regeneration” class to reduce confusion among classes.

Edge Detection Accuracy Compared with Measurement Plots

Boundaries between wetland and other land cover types (upland forest, riparian, and standing water (ponds)) are compared among classification methodologies and geographically located field plot validation in Figure 8. The results of this comparison indicate that all classification methods slightly underestimate wetland extents, on average. The LiDAR-based classification results in the smallest deviation from measured, whereas differences between measured and delineated wetlands are slightly greater, with increasing deviation found among EOSD, AGCC, and measured plot locations. Average LiDAR-classification accuracy for edge detection is -0.3 m (stdev. = 2.3 m from measured), whereas average delineated wetlands from air photos is -1.8 m (stdev. = 8.9 m) from measured. Interestingly, only one wetland boundary was excluded in the LiDAR-based classification, due to confusion with an adjacent road (and therefore no boundary existed), whereas 13 wetland boundaries were excluded in the manual photo delineation, and 29 and 17 of 38 wetland boundaries were misclassified in the EOSD and AGCC classifications, respectively.

Fewer measured plots ($n = 9$) were located between the boundaries of upland forest into treed wetland without some shrub or riparian transition zone. Delineation from air photos compared with measurement plots tended to underestimate wetland boundary (size), thereby extending the boundary of forest into wetland areas by 0.5 m (validation plot $n = 9$), on average, with greater variability (stdev. = 14.2 m), possibly due to vegetation succession or confusion between dark shadows and wetland boundaries (occlusion errors; also found in Chasmer et al. 2014). Average differences between measured plots and wetland-forest boundaries, and the LiDAR classification were -0.3 m (stdev. = 4.6 m), indicating greater ability to differentiate between treed wetland and upland forest. Boundaries between forests and wetlands were often misclassified as forest (conifer, deciduous, or mixed) in the EOSD classification, whereas AGCC

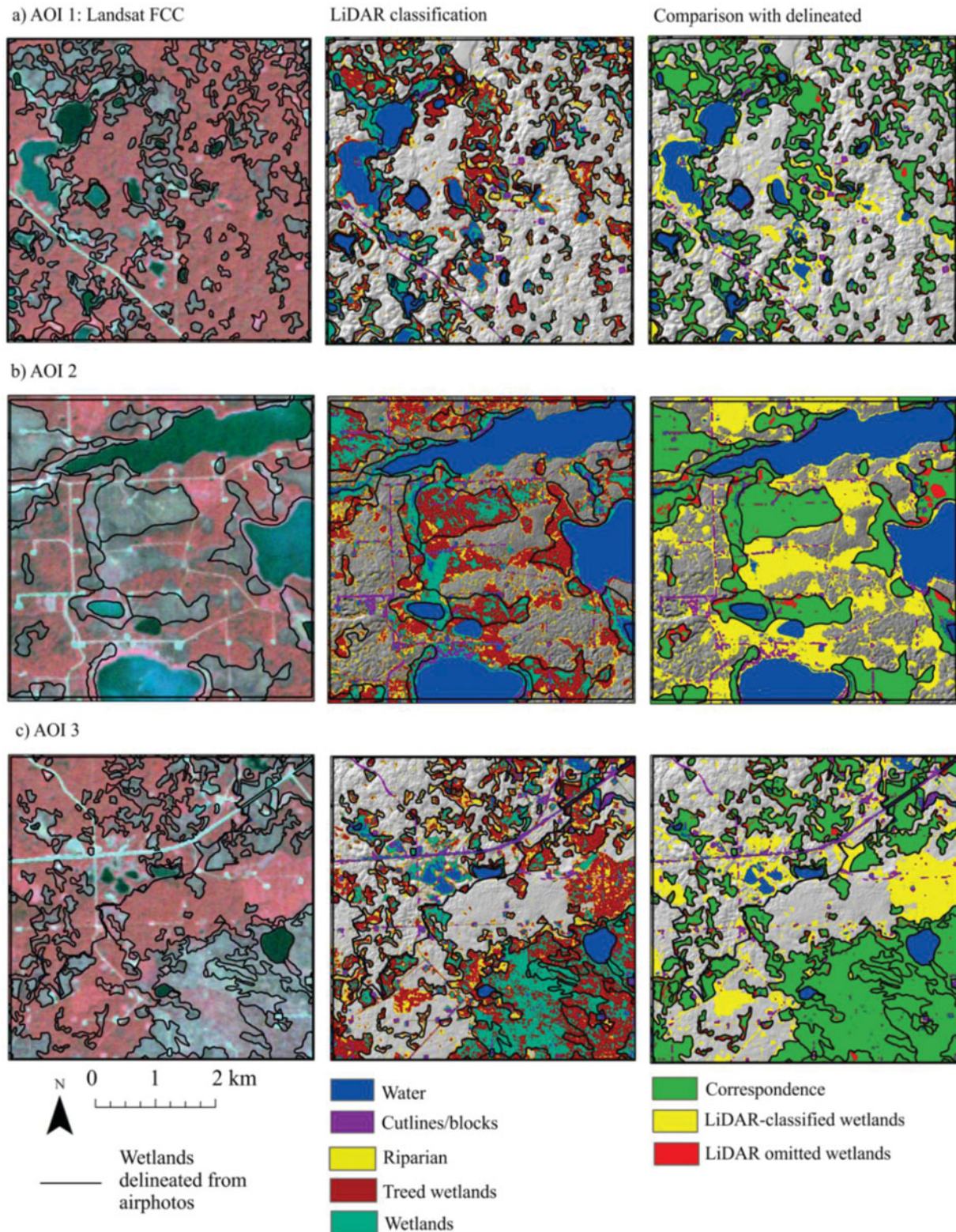


FIG. 7. Comparison of wetland classification within areas of interest illustrating detailed similarities and differences between the LiDAR-based classification and manually delineated wetlands. Landsat TM (2008) false color composite provides visual representation of forested uplands (red) and wetlands (blue/green) with manually delineated wetlands from air photos. Wetlands (including treed and riparian areas) are illustrated in the central panels, with correspondence between classification methods in right panels. A hillshade elevation model illustrates subtle variations in upland topography not classified as wetland.

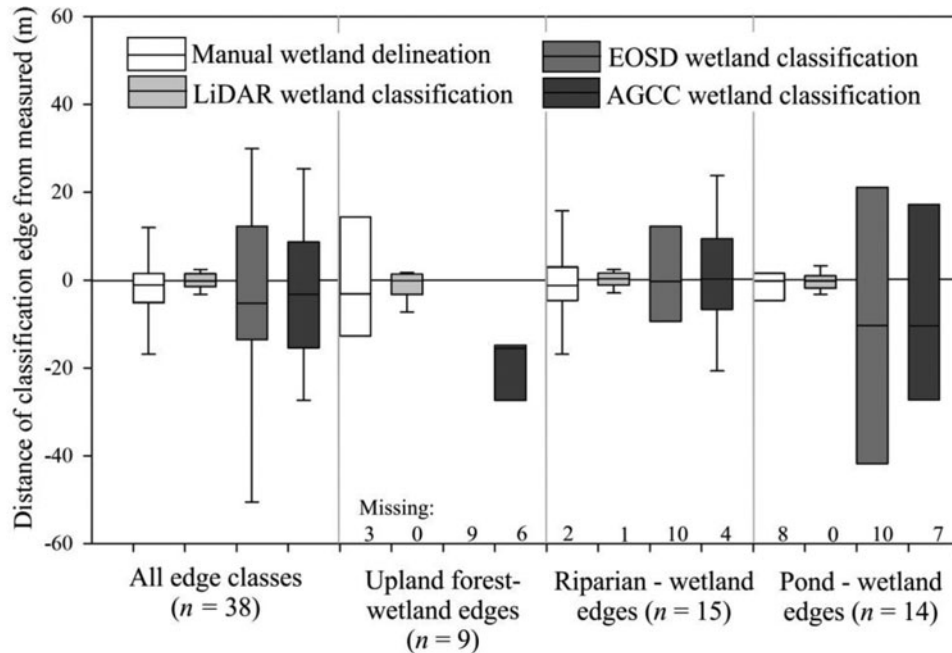


FIG. 8. Box plot of land cover edge detection differences between land cover classifications (manually delineated from air photos, the LiDAR-based classification, EOSD and AGCC) and geolocated plots at land cover boundaries. Zero represents plot measurement location. Negative deviations from measured indicate that the classified boundary is further into the wetland than the measured plot location, whereas positive deviations indicate that the classified boundary extends beyond the measured boundary. The line within the center of the box represents the median, box boundaries indicate the quartile distribution (25th and 75th percentiles) and whisker lines above and below the box indicate 90th and 10th percentiles, respectively.

was able to delineate 3 of 9 boundaries to within -19 m, on average. Riparian to wetland class edge delineation resulted in slight underestimation of wetland size (average = -1.2 m, stdev. = 9.7 m, $n = 15$) based on manually delineated wetlands compared with measurement plots, while LiDAR, EOSD, and AGCC slightly overestimated wetland boundaries: 0.1 m (LiDAR) to 1.3 m (AGCC), moving this further into the riparian zone compared with measured. The standard deviation of offsets from measured clustered within 1.1 m (LiDAR) and 13.3 m (AGCC). One and 2 wetland-riparian boundaries were not classified in the LiDAR-based classification, nor in the manually delineated air photos, and 4 and 10 boundaries were misclassified in AGCC and EOSD datasets. Pond-wetland boundaries, classified using air photo delineation and LiDAR-based methods, have the least variability from measured plot boundaries: stdev. = 2.1 m (LiDAR) and 5.0 m (delineated) of any of the land cover boundary comparisons (forest to wetland, riparian to wetland, pond to wetland). Further, 8 ponds were not delineated separately from wetlands in the air photos, and 10 and 7 ponds were misclassified in the EOSD and AGCC classifications. The range of variability of pond to wetland edge detection using EOSD and AGCC often exceeded the spatial resolution of the classification (25 m), indicating that errors were primarily a result of large mixed pixels that are especially problematic within this heterogeneous region.

DISCUSSION

Use of LiDAR for Mapping Wetlands over Broad Areas

In this study, we present a relatively simple method for classifying wetlands, riparian zones, and ponds, as well as upland mixedwood forests and cutlines/trails roads within the Till Moraine and Clay Plains regions of the Boreal Plains, Alberta. Similarities and differences among LiDAR-based methods, high-resolution air photo delineation of wetlands, field data, and 2 publicly available land cover classifications are also examined. Zoltai and Vitt (1995) describe 5 classes of wetlands that can be formed along complex hydrological, chemical, and biotic criteria, and LiDAR methods may be used to identify proxy indicators from 2 out of 3 of these gradients: hydrological and biotic. Further, Krankina et al. (2008) found that, when examining optical characterization of peatlands, vegetation structure was more important for identifying type than the spectral characteristics of the ground surface. To this end, the characterization and classification of wetland types might depend on a combination of topographic and vegetation-structure derivative products applied in unique ways (Töyra and Pietroniro 2005; Millard and Richardson 2013; Luo et al. 2015) and accuracies could be sufficient enough to require further validation through the use of groundwater chemistry.

The results of this study indicate that the LiDAR-based classification applied to the broad study area accurately corresponds

with 57% of those wetlands that have been manually delineated (based on pixel-to-pixel comparisons; Table 1). This is improved by 5% when confusion due to disturbance is removed. Yet, commission errors account for 37% (total surveyed wetlands, 32% after removal of disturbance-based confusion) of areas classified as wetlands using the LiDAR-based methodology compared with manual photo delineation. Although it is difficult to quantify the numbers of wetlands excluded from the manual delineation of air photos throughout the entire study area (without additional manual delineation from high-resolution optical imagery), proportional areas of missing wetlands range between 16% (with division between Clay Plains and Till Moraine, AOI 3) and 38% (Clay Plains, AOI 2). Photogrammetric methods used to identify wetlands are predisposed to being highly accurate due to high spatial resolution of pixels and care by manual interpreters. Yet, Anderson and Hardin (1992) demonstrate that the detection of wetlands using aerial photographs can be very difficult and might be riddled with error (although current digital methods have vastly improved these methods). Confusion issues include transient or perennial wetland that might not be apparent due to the timing of the photograph, identification of cryptic wetlands (or forested swamps), and differentiating between land surface edges at fuzzy boundaries. Anderson and Hardin (1992) found that 20% of wetlands, including small, forested swamps and perennial wetlands, were excluded from manual delineation of air photos. The use of LiDAR data could also improve wetland classification when compared with photogrammetric methods because both ground surface topography and vegetation characteristics can be included. For example, Creed et al. (2003) were able to automatically identify small cryptic wetlands with convex topographical characteristics more easily than those with shallower edges using airborne LiDAR (but did not compare optical or photogrammetric methods). Forested swamps can also be characterized to some extent using SAR polarimetry (Clark et al. 2009), but are nearly impossible to detect using optical or photogrammetric methods, which are occluded by tree canopies, especially at the edge of the wetland where forest encroachment occurs. Within lower resolution multispectral classification products such as EOSD and AGCC, lower levels of correspondence with the LiDAR classification method (53% and 54%, respectively) are found, including relatively large commission errors (38%). This results in reduced overall wetland areas likely due to mixed pixels and aggregation of land cover types also observed in Frey and Smith (2007).

Within the broader context of the study area (Table 1), LiDAR-based errors of commission are also due, in part, to confusion with areas that have recently undergone some form of disturbance from land use change. Approximately 3% and 5% of Till Moraine and Clay Plains regions have undergone some form of disturbance, and approximately 2/3 of those proportional areas were classified as wetland using LiDAR-based methods (excluding classification of new roads), representing a relatively small proportion of the total area. Regenerating

stands have structural characteristics that are not unlike open wetlands, where flat terrain previously harvested stands contain small shrubs and might be surrounded by upland forests (e.g., characteristics used to define wetlands in Figure 3). These discrepancies require further adjustment to the classification method presented, or inclusion of multitemporal optical data, which increases the complexity and time required to apply the classification. Delineation of harvested stands or inclusion as a separate class requires further development. The fusion of LiDAR and high-resolution optical (multispectral) datasets might improve wetland area and type within a classification, and may be used to differentiate from areas of confusion. For example, rich and poor fens are optically different and may be classified as such because rich fens have an abundance of relatively short sedges, whereas poor fens are dominated by a ground-covering of *Sphagnum* moss. Bubier et al. (1997) and Sonnentag et al. (2007), and others, have found that *Sphagnum* mosses have lower spectral reflectance in the near and shortwave infrared compared with vascular vegetation, and these optical differences can be used to discriminate between rich and poor fens.

Confusion between roads, trails and cutlines, and wetland classes determined from LiDAR-based methods (34% commission errors compared with EOSD, Table 1) often occur in areas where cut lines and trails traverse wetlands, or are topographically low lying compared with nearby elevations (also found when compared to an individual plot measurement of wetland edge, Figure 8). In some areas, small wetlands form where cut lines, trails, and roads once stood or are currently used (observed while doing field work, but not georegistered). Smerdon et al. (2009) note that the effect of roads on hydrology in the Boreal Plains depends on landscape position and underlying geology as well as the location of groundwater recharge and discharge areas. Quantifying the true area extent and number of roads and trails that have this saturated ground/wetland appearance is difficult to determine using field methods alone due to accessibility and the perennial nature of some of these saturated areas. Future development of a LiDAR-based wetland classification might incorporate linear features (roads, paths, etc.) that could be more or less prone to flooding and hydrologically sensitive adjacent land areas. This could provide information services for future planning and resources extraction.

Implications of Accurate Wetland Edge Detection

One of the most critical components of wetland classification is the ability to accurately characterize wetland edges and transition zone boundaries needed for baseline assessments, change detection, and monitoring. These requirements are also defined within wetland classes of publicly available datasets (Level 4 – EOSD, Wulder et al. 2006; Level 2 – AGCC, Sánchez-Azofeifa et al. 2005). Comparisons among LiDAR-based classification methods used in this study and geographically located measurement plots found along wetland and transition zone boundaries (upland forest, riparian zone, and standing water in ponds)

indicate close correspondence (-0.3 m on average), and reduced residual variability between wetland edges and measured plots (Figure 8). All classification methods underestimate wetland extent, on average, compared with plot boundaries. Average manually delineated offsets were -1.8 m, and these increased to -3.9 m and -4.0 m, on average, for EOSD and AGCC, respectively; whereas variability in edge location from measured increased significantly among LiDAR-based methods, delineated photographs, to EOSD, with a slight improvement by using AGCC for wetland edge detection. Timing between data collection (aerial photography, Landsat imagery, and LiDAR survey) might also result in slight offsets of classified wetland boundaries compared with measured plots. For example, boundaries between wetland edges and ponds ($n = 14$) were underestimated by -1.1 m and -0.3 m (manual delineation and LiDAR methods, respectively), indicating that water levels might have been higher, with greater wetland encroachment, during the LiDAR survey as a result of greater-than-average annual and summer precipitation in 2007 and 2008 (Petroni et al. 2014).

With regard to increased offset variability in manually delineated air photos compared at upland forest and riparian zone-wetland edges, this could have been caused, in part, by occlusion at transitional or fuzzy boundaries. For example, dense riparian vegetation can mask subtle changes in topography that might be used to identify depressions, while shadows cast by taller vegetation at wetland edges could be confused with tree canopies, resulting in underestimation of wetland area, depending on sun angles at the time of photo overpass (Chasmer et al. 2011). Wetland boundaries determined by AGCC and EOSD also suffer from mixed-pixel influences where greater proportional coverage (and spectral reflectance) will be from forest and/or riparian zones. The width of riparian to open wetland to pond land cover types can vary by as little as 5 m, and can extend to 50 m in some areas. Within narrow or small wetlands, EOSD and AGCC are more prone to misclassification errors and larger edge residuals as a result of mixed pixels when compared with measured (Figure 8). Often, small wetlands are missed entirely, resulting in 76% of misclassification errors based on EOSD compared with measurement plots (Figure 8); although misclassification is reduced as wetland size increases beyond an area equal to several Landsat pixels. The results shown here demonstrate the importance of spatial pixel resolution on the accuracy of wetland edge detection. Similarity between average and residual differences between plot measured, LiDAR, and photogrammetric-based classification methods also indicate that, although photogrammetric methods are relatively accurate for delineating wetland extents and types, missed wetlands and inclusion of ponds within wetland classes can either under- or overestimate the extent of wetlands within a given area. LiDAR provides a cost-effective method for broad-area mapping where available, and especially in heterogeneous regions that could be difficult to accurately characterize using lower-resolution multispectral classification methods or time-consuming photogrammetric delineation.

Applicability of the LiDAR Wetland Classification for Provincial Monitoring

The LiDAR-based classification described in this study differs from empirical “black box” or machine learning methods, which depend on the ranking of a series of simple to complex statistical relationships among up to hundreds of discrete and/or continuous datasets (Pal 2005). Empirical methods also assume that the full range of characteristics within the area to be classified have been identified and represented within the reference training data and, therefore, require substantial reference data to run models. If the model is applied to other regions that have not been appropriately characterized by training data, the accuracy of the classification will be significantly reduced (Vauhkonen et al. 2010). For forest species discrimination requiring tree-level measurements, National Forest Inventory (NFI) data may be used, as long as the data provide enough information required by the model (e.g., Vauhkonen et al. 2010); alternatively, other training data may be used to drive empirically based models. However, datasets need to consistently measure the same variables to be used in the model, and additional classification areas require new training data, while greater complexity of environmental characteristics would require additional training data (Vauhkonen et al. 2010). In areas where extensive training data exist or can be created, empirical methods can be highly effective (Millard and Richardson 2013), and even more so than traditional methods of classification, because they exploit information inherent in the LiDAR point clouds that might be lost by using grid-based layers (Zhao et al. 2011), albeit Millard and Richardson (2013) found that most layers co-vary and only a handful of data derivatives might be used to drive the model.

With regard to model complexity, data derivatives, and storage, single-band raster (LiDAR) datasets and derivatives used in this study are 1.76 GB each for the 1,036-km area. Further, 2,330 (delineated) wetlands are examined using a variety of classifications. For comparison, Millard and Richardson (2013) included over 120 input channels with a total disk size of ~ 400 MB in a Random Forest classification of ~ 28 km². Data layers were used to characterize wetland features within a bog and surrounding land cover types, with high accuracy. Provincial application of such a model would require significant consideration of computer and space resources for an area exceeding 650,000 km² (the total area of Alberta). This suggests that a trade-off exists among data derivatives, training constraints, and classification methodologies such that the cost and complexity of applications need to be carefully considered. Simplicity of wide-area mapping methods and movement away from more complex methods of classification have been discussed in Korpela et al. (2009) and Vauhkonen et al. (2010), although LiDAR methods can only be used to map structure. The need to quantify vegetation species types requires the use of optical imagery (Korpela et al. 2009) or might show promise through multispectral LiDAR. Although decision-making criteria for the physical environment, such as

those applied in this study, might be difficult to initialize, the collection of all permutations of the physical environment required for more complex models could be equally difficult. The use of a single dataset for classification is also operationally beneficial for reducing the cost of purchasing additional data and storage, as well as the added complexity associated with the management and processing of other remote sensing datasets over broad areas (Korpela et al. 2009), as long as the method is accurate and suitable for the application.

The performance of the classification presented in this study will also likely require reevaluation of wetland fingerprints as methods are extended into other ecozones such as the prairie pothole/grassland regions of the agricultural zones, aspen parkland, etc., but these might require adjustment of only the classes used to divide current inputs, opposed to the organization of new data derivatives. This also reduces the need for significant space and computer resources required by more complex models such as Random Forest, and might also indicate universality between important inputs and data derivatives such as all-return variance for defining wetlands. Application and testing across other wetland ecosystems with the use of additional field data for validation in the future will contribute to better quantification of the extent of wetlands in Alberta as baseline, and an important step toward accurate provincial wetland mapping requirements of the Alberta Wetland Policy.

CONCLUSIONS

In this study, we present a relatively simple LiDAR-based decision classification of topographical variation above/below the mean surface, depending on surface variability, and the variance of vegetation structural characteristics found within all returns of the LiDAR dataset for a moderately sized Boreal Plains region of western Canada. The results of this study indicate that our methods can be applied to delineate wetland extent and features at or exceeding the accuracy of manually delineated air photos. Errors of commission were 32% (after correcting for harvest) and omission were 6%, on average, with relatively high commission errors as a result of misclassification in the manually delineated air photo dataset. Further, the LiDAR-based classification took less than 1 day to apply (although data derivative products took considerably longer—up to 2 weeks—to create), while air photo delineation can take hours to many months or longer, depending on the size of the area delineated and the number photo interpreters. When compared with publicly available datasets AGCC and EOSD, we found that wetlands in both classifications (including the delineated air photos) were excluded as a result of coarse pixel resolution. Further, many wetlands were missed in the air photo delineation, and, in some areas, ponds were included within the wetland class. This suggests significant underestimation of the extent and numbers of wetlands in this region using photo interpretation and multispectral methods. In the case of the LiDAR-based classification, this result is also complicated by previously clearcut and regener-

ating forest stands that have similar structural and topographic characteristics to wetlands.

Future research on the use of LiDAR for wetland delineation and type classification should consider the effects of survey timing and seasonality on classification accuracy with regard to soil saturation and water table position above the ground surface, as well as the ability to quantify vegetation structural characteristics surveyed using LiDAR during shoulder periods (Wasser et al. 2013). This is of relevance for wide-area provincial, state, and national initiatives, which often parameterize surveys for accurate acquisition of ground elevation, but are less interested in vegetation. The defining characteristics used to identify wetland classes might require adjustment for phenology at the time of survey, in addition to reassessment of characteristics as they vary across ecozones and subregions.

ACKNOWLEDGMENTS

The authors would like to thank 3 anonymous reviewers for their helpful suggestions to improve this manuscript and discussions with Dr. Bob Sleep. We also acknowledge field assistance from Dr. Gabor Sass, Stella Heenan, Ron Chasmer, and Dr. John Barlow (with Chasmer and Hopkinson in 2002), Scott Brown (2008), Kayla Heath (with Hopkinson in 2012), Reed Parsons, and Mark Derksen (with Chasmer and Hopkinson in 2015). Airborne LiDAR data was surveyed by Airborne Imaging Inc. (Calgary), licensed to the Government of Alberta, and organized for use by Drs. Shane Patterson and Brett Purdy. Publicly available EOSD data were acquired from the Canadian Forest Service, and AGCC was provided by the Government of Alberta. Delineated wetlands were provided by the Devonian Institute, University of Alberta. Multitemporal Landsat MSAVI data were obtained from Earth Explorer. SPOT 5 and WorldView-2 data were obtained from Blackbridge Inc., Lethbridge AB. We also acknowledge Dr. Kevin Devito (site PI) for continued support and access to the Utikuma Regional Study Area.

FUNDING

Postdoctoral funding to Laura Chasmer was provided by Alberta Innovates Technology Futures. Funding for this project has been supported by the Canadian Foundation for Innovation, Natural Sciences Engineering Research Council Discovery Grant, and Campus Alberta provided to Dr. Chris Hopkinson.

REFERENCES

- Anderson, V.J., and Hardin, P.J. 1992. "Infrared photo interpretation of non-riparian wetlands." *Rangelands*, Vol. 14(No. 6): pp. 334–337.
- Bubier, J.L., Rock, B.N., and Crill, P.M. 1997. "Spectral reflectance measurements of boreal wetland and forest mosses." *Journal of Geophysical Research - Atmospheres*, Vol. 102: pp. 29483–29494.
- Chasmer, L., Hopkinson, C., and Quinton, W. 2011. "Quantifying errors in permafrost plateau change from optical data, Northwest Territories, Canada: 1947 to 2008." *Canadian Journal of Remote Sensing – CRSS Special Issue*, Vol. 36(No. 2): pp. S211–S223.

- Chasmer, L., Hopkinson, C., Quinton, W., Veness, T., and Baltzer, J. 2014. "A decision-tree classification for low-lying complex land cover types within the zone of discontinuous permafrost." *Remote Sensing of Environment*, Vol. 143: pp. 73–84.
- Clark, R.B., Creed, I.F., and Sass, G.Z. 2009. "Mapping hydrologically sensitive areas on the Boreal Plain: a multitemporal analysis of ERS synthetic aperture radar data." *International Journal of Remote Sensing*, Vol. 30(No. 10): pp. 2619–2635.
- Crauto, N., Hopkinson, C., Forbes, D.L., Lesack, L., Marsh, P., Spooner, I., Van Der Sanden, J.J. 2015. "A LiDAR-based decision-tree classification of open water surfaces in an Arctic delta." *Remote Sensing of Environment*, Vol. 164: pp. 90–102.
- Creed, I.F., Sanford, S.E., Beall, F.D., Molot, L.A., and Dillon, P.J., 2003. "Cryptic wetlands: integrating hidden wetlands in regression models of the export of dissolved organic carbon from forested landscapes." *Hydrological Processes*, Vol. 17: pp. 3629–3648.
- de Groot, W.J., Flannigan, M.D., and Cantin, A.S. 2013. "Climate change impacts on future boreal fire regimes." *Forest Ecology and Management*, Vol. 294: pp. 35–44.
- Devito K.J., Creed, I.F., and Fraser, C. 2005. "Controls on runoff from a partially harvested aspen forested headwater catchment, Boreal Plain, Canada." *Hydrological Processes*, Vol. 19: pp. 3–25.
- Ducks Unlimited Canada. 2002. *Utikuma Lake, Alberta Earth Cover Classification User's Guide*. Edmonton, AB, Canada/Rancho Cordova, CA, USA: Ducks Unlimited, Inc.
- Environment Canada. 2016. <https://www.ec.gc.ca/eau-water/default.asp?lang=En&n=27147C37-1>. Accessed July 2, 2016.
- Ferone, J. M., and Devito, K.J. 2004. "Shallow groundwater-surface water interactions in pond-peatland complexes along a Boreal Plains topographic gradient." *Journal of Hydrology*, Vol. 292: pp. 75–95.
- Frey, K.E. and Smith, L.C., 2007. "How well do we know northern land cover? Comparison of four global vegetation and wetland products with a new ground-truth database for West Siberia." *Global Biogeochemical Cycles*, Vol. 21: pp. GB1016. doi:10.1029/2006GB002706.
- Gilmore, M.S., Wilson, E.H., Barrett, N., Civco, D.L., Prisløe, S., Hurd, J.D., and Chadwick, C. 2008. "Integrating multi-temporal spectral and structural information to map wetland vegetation in a lower Connecticut River tidal marsh." *Remote Sensing of Environment*, Vol. 112: pp. 4048–4060.
- Government of Alberta. 2013. *Alberta Wetland Policy*. <http://aep.alberta.ca/water/programs-and-services/wetlands/documents/AlbertaWetlandPolicy-Sep2013.pdf>. Accessed October 13, 2015.
- Hall, O., and Hay, G.J. 2003. "Multiscale object-specific approach to digital change detection." *International Journal of Applied Earth Observation and Geoinformation*, Vol. 4: pp. 311–327.
- Halsey, L.A., Vitt, D.H., Beilman, D., Crowand, S., and Wells, S.M. R., 2003. *Alberta Wetlands Classification System, v. 2.0*. Edmonton, AB, Canada: Government of Alberta, Alberta Sustainable Resource Development.
- Halsey, L.A., Vitt, D.H., Beilman, D., Crow, S., Mehelcic, S., and Wells, R. 2004. *Alberta Wetland Inventory Classification System, version 2.0*. Pub # T/031. Edmonton, AB, Canada: Government of Alberta, Alberta Sustainable Resource Development.
- Hogg, A.R., and Todd, K.W. 2007. "Automated discrimination of upland and wetland using terrain derivatives." *Canadian Journal of Remote Sensing*, Vol. 33(No. 1): pp. S68–S83.
- Hopkinson, C. 2007. "The influence of flying altitude, bean divergence, and pulse repetition frequency on laser pulse return intensity and canopy frequency distribution." *Canadian Journal of Remote Sensing*, Vol. 33(No. 4): pp. 312–324.
- Hopkinson, C., Chasmer, L., Colville, D., Fournier, R., Hall, R.J., Luther, J.E., Milne, T., Petrone, R., and St-Onge, B. 2013. "Moving toward consistent ALS monitoring of forest attributes across Canada: A consortium approach." *Photogrammetric Engineering and Remote Sensing*, Vol. 79(No. 2): pp. 159–173.
- Hopkinson, C., Chasmer, L., Lim, K., Treitz, P., and Creed, I. 2006. "Towards a universal LiDAR canopy height indicator." *Canadian Journal of Remote Sensing*, Vol. 32(No. 2): pp. 139–152.
- Hopkinson, C., Chasmer, L., Sass, G., Creed, I., Sitar, M., Kalbfleisch, W., and Treitz, P. 2005. "Vegetation class dependent errors in lidar ground elevation and canopy height estimates in a boreal wetland environment." *Canadian Journal of Remote Sensing*, Vol. 31(No. 2): pp. 191–206.
- Klein, E., Berg, E.E., and Dial, R. 2005. "Wetland drying and succession across the Kenai Peninsula Lowlands, south-central Alaska." *Canadian Journal of Forest Research*, Vol. 35: pp. 1931–1941.
- Knight, J.F., Tolcser, B.P., Corcoran, J.M., and Rampi, L.P., 2013. "The effects of data selection and thematic detail on the accuracy of high spatial resolution wetland classifications." *Photogrammetric Engineering and Remote Sensing*, Vol. 79(No. 7): pp. 613–623.
- Komers, P.E., and Stanojevic, Z. 2013. "Rates of disturbance vary by data resolution: implications for conservation schedules using the Alberta Boreal Forest as a case study." *Global Change Biology*, Vol. 19: pp. 2916–2928.
- Korpela, I., Koskinen, M., Vasander, H., Holopainen, M., and Minkkinen, K. 2009. "Airborne small-footprint discrete-return LiDAR data in the assessment of boreal mire surface patterns, vegetation, and habitats." *Forest Ecology and Management*, Vol. 258: pp. 1549–1566.
- Krankina, O.N., Pflugmacher, D., Friedl, M., Cohen, W.B., Nelson, P., and Baccini, A., 2008. "Meeting the challenge of mapping peatlands with remotely sensed data." *Biogeosciences*, Vol. 5: pp. 1809–1820.
- Luo, S., Wang, C., Pan, F. Xi, X., Li, G., Nie, S., and Xia, S. 2015. "Estimation of wetland vegetation height and leaf area index using airborne laser scanning data." *Ecological Indicators*, Vol. 48: pp. 550–559.
- Masek, J.G., Vermote, E.F., Saleous, N., Wolfe, R., Hall, F.G., Huemmrich, F., Gao, F., Kutler, J., and Lim, T.K. 2006. "A Landsat surface reflectance data set for North America, 1990–2000." *IEEE Geoscience and Remote Sensing Letters*, Vol. 3: pp. 68–72.
- Millard, K., and Richardson, M. 2013. Wetland mapping with LiDAR derivatives, SAR polarimetric decompositions, and LiDAR-SAR fusion using a random forest classifier. *Canadian Journal of Remote Sensing*, Vol. 39(No. 4): pp. 290–307.
- Morsdorf, F., Frey, O., Meier, E., Itten, K.J., and Allgöwer, B. 2008. "Assessment of the influence of flying altitude and scan angle on biophysical vegetation products derived from airborne laser scanning." *International Journal of Remote Sensing*, Vol. 29(No. 5): pp. 1387–1406.
- National Wetlands Working Group. 1988. *Wetlands of Canada*. Ecological Land Classification Series, No. 24. Sustainable Development Branch, Environment Canada, Ottawa Ontario. Montreal, Quebec, Canada: Polyscience Publications Inc.
- National Wetlands Working Group. 1997. *The Canadian Wetland Classification System: A Revision of the Wetlands of Canada*, edited by

- B.G. Warner and C.D.A. Rubec. Ontario, Canada: Wetlands Research Centre, University of Waterloo.
- Natural Regions Committee. 2006. *Natural Regions and Subregions of Alberta*. Pub # T/852. Compiled by D.J. Downing and W.W. Pettapiece. Government of Alberta. http://www.cd.gov.ab.ca/preserving/parks/ahic/Natural_region_report.asp. Accessed June 25, 2015.
- Ozesmi, S.L., and Bauer, M.E. 2002. "Satellite remote sensing of wetlands." *Wetlands Ecology and Management*, Vol. 10: pp. 381–402.
- Pal, M. 2005. "Random forest classifier for remote sensing classification." *International Journal of Remote Sensing*, Vol. 26(No. 1): pp. 217–222.
- Petrone, R., Chasmer, L., Hopkinson, C., Silins, U., Landhausser, S., Kljun, N., Devito, K.J. 2014. "Effects of harvesting on CO₂ and H₂O fluxes during wet and dry years in an aspen dominated Western Boreal Plain Forest." *Canadian Journal of Forest Research*, Vol. 45: pp. 87–100.
- Petrone, R.M., Silins, U., and Devito, K.J., 2007. "Dynamics of evapotranspiration from a riparian pond complex in the Western Boreal Forest, Alberta, Canada." *Hydrological Processes*, Vol. 21: pp. 1391–1401.
- Richardson, M.C., Mitchell, C.P.J., Branfireun, B.A., and Kolka, R.K. 2010. "Analysis of airborne LiDAR surveys to quantify the characteristic morphologies of northern forested wetlands." *Journal of Geophysical Research – Biogeosciences*, Vol. 115(No. G3), G03005, 16 pg. doi: 10.1029/2009JG000972.
- Riordan, B., Verbyla, D., and McGuire, A.D. 2006. "Shrinking ponds in subarctic Alaska based on 1950–2002 remotely sensed images." *Journal of Geophysical Research*, Vol. 111: pp. G04002.
- Roulet, N.T. 2000. "Peatlands, carbon storage, greenhouse gases, and the Kyoto protocol, prospects and significance for Canada." *Wetlands*, Vol. 20: pp. 605–615.
- Sánchez-Azofeifa, G.A., Chong, M., Sinkwich, J., and Mamet, S. 2004. *Alberta Ground Cover Characterization (AGCC) Training and Procedures Manual*. Edmonton, Alberta, Canada: University of Alberta.
- Smith, A.M.S., Kolden, C.A., Tinkham, W.T., Talhelm, A.F., Marshall, J.D., Hudak, A.T., Boschetti, L., et al. 2014. "Remote sensing the vulnerability of vegetation in natural terrestrial ecosystems." *Remote Sensing of Environment*, Vol. 154: pp. 322–337.
- Sonnentag, O., Chen, J.M., Roberts, D.A., Talbot, J., Halligan, K.Q., Govind, A. 2007. "Mapping tree and shrub leaf area indices in an ombrotrophic peatland through multiple endmember spectral unmixing." *Remote Sensing of Environment*, Vol. 109(No. 3): pp. 342–360.
- Stow, D.A., Hope, A. McGuire, D. Verbyla, D., Gamon, J., Huemmrich, F., Houston, S., et al. 2004. "Remote sensing of vegetation and land-cover change in Arctic tundra ecosystems." *Remote Sensing of Environment*, Vol. 89(No. 3): pp. 281–308.
- Sturm, M., Racine, C., and Tape, K. 2001. "Increasing shrub abundance in the Arctic." *Nature*, Vol. 411: pp. 546–547.
- Tarnocai, C. 2009. "The impact of climate change on Canadian peatlands." *Canadian Water Resources Journal*, Vol. 34(No. 4): pp. 453–466.
- Töyra, J., and Pietroniro, A. 2005. "Towards operational monitoring of a northern wetland using geomatics-based techniques." *Remote Sensing of Environment*, Vol. 97: pp. 174–191.
- Vauhkonen, J., Korpela, I., Maltamo, M., Tokola, T. 2010. "Imputation of single-tree attributes using airborne laser scanning-based height, intensity, and alpha shape metrics." *Remote Sensing of Environment*, Vol. 114: pp. 1263–1276.
- Vitt, D.H., Halsey, L.A., Thormann, M.N., and Martin, T. 1996. *Peatland Inventory of Alberta*. Edmonton, Alberta, Canada: National Centers of Excellence in Sustainable Forest Management, University of Alberta.
- Wasser, L., Day, R., Chasmer, L., and Taylor, A. 2013. "Influence of vegetation structure on lidar-derived canopy height and fractional cover in forested riparian buffers during leaf-off and leaf-on conditions." *PLoS ONE*, Vol. 8(No. 1): pp. e54776. doi:10.1371/journal.pone.0054776.
- White, B., Ogilvie, J., Campbell, D.M.H., Hiltz, D., Gauthier, B., Chisholm, K., Wen, H.K., Murphy, P.N.C. and Arp, P. 2012. "Using the cartographic depth-to-water index to locate small streams and associated wet areas across landscapes." *Canadian Water Resources Journal*, Vol. 37(No. 4): pp. 333–347.
- Wulder, M.A., White, J.C., Luther, J.E., Strickland, G., Rimmel, T.K., and Mitchell, S.W. 2006. "Use of vector polygons for the accuracy assessment of pixel-based land cover maps." *Canadian Journal of Remote Sensing*, Vol. 32(No. 3): pp. 268–279.
- Wulder, M.A., White, J.C., Magnussen, S., and McDonald, S. 2007. "Validation of a large area land cover product using purpose-acquired airborne video." *Remote Sensing of Environment*, Vol. 106(No. 4): pp. 480–491.
- Wulder, M.A., White, J.C., Cranny, M., Hall, R.J., Luther, J.E., Beaudoin, A., Goodenough, D. G., and Dechka, J.A. 2008. "Monitoring Canada's forests. Part 1: Completion of the EOSD land cover project." *Canadian Journal of Remote Sensing*, Vol. 34(No. 6): pp. 549–562.
- Zoltai, S.C. and Vitt, D.H. 1995. "Canadian wetlands: Environmental gradients and classification." *Vegetation*, Vol. 118: pp. 131–137.
- Zhao, K., Popescu, S., Meng, X., Pang, Y., and Agca, M. 2011. "Characterizing forest canopy structure with LiDAR composite metrics and machine learning." *Remote Sensing of Environment*, Vol. 115: pp. 1978–1996.